



Archived by Flinders University

This is the peer reviewed version of the following article:

Irvine, D. J., Werner, A. D., Ye, Y., & Jazayeri, A. (2020).  
Upstream Dispersion in Solute Transport Models: A  
Simple Evaluation and Reduction Methodology.  
*Groundwater*, 59(2), 287–291.

which has been published in final form at

<https://doi.org/10.1111/gwat.13036>

This article may be used for non-commercial purposes in  
accordance with Wiley Terms and Conditions for self-  
archiving.

Copyright © 2020 John Wiley & Sons, Inc.

All rights reserved.

## **Methods Note:**

### **Upstream dispersion in solute transport models: A simple evaluation and reduction methodology**

D.J. Irvine<sup>1\*</sup>, A.D. Werner<sup>1</sup>, Y. Ye<sup>2</sup>, A. Jazayeri<sup>1</sup>

<sup>1</sup>College of Science and Engineering, and National Centre for Groundwater Research and Training, Flinders University, Adelaide, Australia.

<sup>2</sup>State Key Laboratory of Hydrology-Water Resources and Hydraulic Engineering, Hohai University, Nanjing, China.

\*Corresponding author: [dylan.irvine@flinders.edu.au](mailto:dylan.irvine@flinders.edu.au)

## **Paper type**

Methods note

## **Article impact statement**

We derive 1D analytical solutions to quantify, and provide a simple approach to reduce, upstream dispersion in solute transport models.

1 **Abstract**

2

3 This article outlines analytical solutions to quantify the length scale associated with “upstream  
4 dispersion”, the artificial movement of solutes in the opposite direction to groundwater flow, in  
5 solute transport models. Upstream dispersion is an unwanted artefact in common applications of  
6 the advection-dispersion equation (ADE) in problems involving groundwater flow in the direction  
7 of increasing solute concentrations. Simple formulae for estimating the one-dimensional distance  
8 of upstream dispersion are provided. These show that under idealized conditions (i.e., steady-state  
9 flow and transport, and a homogeneous aquifer), upstream dispersion may be a function of only  
10 longitudinal dispersivity. The scale of upstream dispersion in a selection of previously presented  
11 situations is approximated to highlight the utility of the presented formulae and the relevance of  
12 this ADE anomaly in common transport problems. Additionally, the analytical solution is applied  
13 in a hypothetical scenario to guide the modification of dispersion parameters to minimize upstream  
14 dispersion.

15

16 **Introduction**

17

18 The traditional application of the advection-dispersion equation (ADE) to macroscopically  
19 homogeneous aquifers often produces qualitatively dissimilar results to the contaminant transport  
20 observed in laboratory experiments and field-scale tests (e.g., Di Donato et al. 2003). One example  
21 of unexpected solute transport behavior is caused by upstream dispersion, which occurs when  
22 groundwater flows towards a solute source (Konikow 2011). Under these conditions, the  
23 concentration and hydraulic gradients are in opposite directions, leading to dispersive mass fluxes

24 against the direction of flow. Upstream dispersion is an unwanted artefact in simulations of solute  
25 transport that are caused by the Fickian dispersion model that underpins the ADE, which assumes  
26 that the concentration gradient is the driving force for solute spreading (e.g., Konikow 2011). Mass  
27 fluxes in the opposite direction to fluid flow only occur in real-world situations when molecular  
28 diffusion is in excess of the advective flux, e.g., as may occur in aquitards (e.g., Barbour et al.  
29 2012; Zhang et al. 2015; Knight et al. 2019).

30  
31 Upstream dispersion has been noted as an issue in several investigations aimed at quantifying  
32 macro-scale solute transport and involving groundwater flow in the direction of increasing solute  
33 concentration. Here, the term “macro-dispersion” refers to values of dispersion adopted in real-  
34 world problems, where the action of heterogeneity is implicit in field-scale dispersion coefficients,  
35 as described by Cvetkovic (2013). Documented examples of problems where upstream dispersion  
36 is apparent include: groundwater discharge towards saltwater boundaries (Henry 1964; Wooding  
37 et al. 1997), solute transport in aquifers containing structured heterogeneities, including faults and  
38 fractures (Robinson et al. 1998; Liu et al. 2004; Sebben and Werner 2016), forced-tracer tests  
39 (Chen et al. 1996), and solute exchange between the surface and subsurface domains of hillslope  
40 settings (Liggett et al. 2014). Despite its frequent occurrence, no attempt has been made to provide  
41 an approach to estimate the scale of upstream dispersion.

42  
43 This study uses an intentionally simple conceptualization of one-dimensional (1D), steady-state  
44 fresh groundwater flow towards a solute source to quantify upstream dispersion under idealized  
45 conditions. In this study, we: (1) derive analytical solutions to quantify upstream dispersion for  
46 simple conditions; (2) apply these analytical solutions to previously published examples of

47 situations where upstream dispersion is expected to occur; and (3) describe a simple approach to  
48 reduce upstream dispersion in solute transport simulations.

49

## 50 **Materials and Methods**

51

### 52 **Theory and Analytical Solution Derivation**

53

54 The ADE for 1D non-reactive solute transport in a steady groundwater flow field is:

$$55 \quad D_L \frac{\partial^2 C}{\partial x^2} - v \frac{\partial C}{\partial x} = \frac{\partial C}{\partial t} \quad (1)$$

56

57 where  $C$  is concentration [ $\text{ML}^{-3}$ ],  $v$  is average linear velocity [ $\text{LT}^{-1}$ ],  $t$  is time [ $\text{T}$ ], and  $x$  is position  
58 [ $\text{L}$ ], positive in the direction of groundwater flow. The hydrodynamic dispersion coefficient  $D_L$   
59 [ $\text{L}^2\text{T}^{-1}$ ] includes both molecular diffusion,  $D_m$  [ $\text{L}^2\text{T}^{-1}$ ], and mechanical dispersion, whereby the  
60 latter represents the mechanical mixing. That is,  $D_L = D_m + \alpha_L v$ , where  $\alpha_L$  is the longitudinal  
61 dispersivity [ $\text{L}$ ].  $D_m$  is proportional to the aqueous diffusion coefficient,  $D_{\text{aq}}$  [ $\text{L}^2\text{T}^{-1}$ ], and is affected  
62 by the porosity and the tortuosity of the porous medium.

63

64 The left side of Equation 1 is related to the solute mass flux gradient,  $-\partial J/\partial x$ , where  $J$  [ $\text{MT}^{-1}\text{L}^{-2}$ ] is  
65 the diffusive solute flux per unit area (i.e., the solute mass flux divided by the cross-sectional area  
66 to flow and divided by porosity). Therefore, under steady-state solute conditions ( $\partial C/\partial t = 0$ ),  $J$  is  
67 a constant obtained by solving the partial differential Equation 1:

$$68 \quad J = vC - e^{\frac{v}{D_L}(x+E)} \quad (2)$$

69

70 Here,  $J$  and the integration constant  $E$  are found from knowledge of the solute boundary conditions.

71 In our case, the downstream efflux boundary is represented by a Dirichlet boundary conditions

72 (Type 1) of specified solute concentration,  $C_2$ , to create the situation of freshwater flow in the

73 direction of increasing concentration. The upstream boundary might commonly be treated as

74 either: (A) a Dirichlet boundary conditions (Type 1) of specified concentration  $C_1$ , or (B) a Cauchy

75 boundary condition in which  $J$  is specified as  $J_0$ . Equations 3 and 4 are easily obtained by applying

76 the boundary condition from Case A to Equation 2, as:

77

$$J = vC_1 - \frac{v(C_2 - C_1)}{\left( e^{\frac{vL}{D_L}} - 1 \right)}, \quad (3)$$

78

$$C = C_1 + (C_2 - C_1) \frac{\left( e^{\frac{vx}{D_L}} - 1 \right)}{\left( e^{\frac{vL}{D_L}} - 1 \right)}. \quad (4)$$

79

80 Applying Case B boundary conditions produces the following solution:

81

$$C = \left( C_2 - \frac{J_0}{v} \right) e^{\frac{v(x-L)}{D_L}} + \frac{J_0}{v}, \quad (5)$$

82

83 where  $L$  is length of the model domain [L]. In situations where the conceptualized value of  $J$ , given

84 in Equation 3, is the specific mass flux through the boundary, given by  $vC_1$ , then the departure

85 from this value is the second term on the right-hand side of Equation 3. The differences in mass

86 flux and solute concentrations between the two boundary condition cases are larger for smaller

87 values of the Péclet number,  $Pe$  [-], which is  $vL/D_L$ .

88

89 The extent of upstream dispersion is defined here as the upstream distance,  $F$  [L], to a prescribed  
90 solute concentration, given as  $C_F$  [-]. Adopting Case A boundary conditions, and with  $C_1$  and  $C_2$   
91 taken as 0 and 1, respectively, leads to:

$$92 \quad F = L - \frac{D_L}{v} \ln \left( C_F e^{\frac{vL}{D_L}} - C_F + 1 \right). \quad (6)$$

93

94 Case B boundary conditions, with  $J_0$  and  $C_2$  taken as 0 and 1, respectively, produces:

$$95 \quad F = -\frac{D_L}{v} \ln C_F. \quad (7)$$

96

97 In cases where  $D_m \ll \alpha_L v$ , upstream dispersion is controlled by  $\alpha_L$  and  $L$  where Case A boundary  
98 conditions are imposed, whereas upstream dispersion is a function of only  $\alpha_L$  under Case B  
99 boundary conditions, according to Equations 6 and 7, respectively. The value of  $F$  from Equation  
100 6 increases asymptotically towards that obtained from Equation 7 as  $L$  increases. Further  
101 simplifications of Equation 7 are possible if the following assumptions are made:  $\alpha_L$  is taken as  
102  $0.1L$  (Gelhar et al. 1992), notwithstanding other factors and available functions relating  $\alpha_L$  to  $L$   
103 (e.g., Neuman 1990; Xu and Eckstein 1995; Schulze-Makuch 2005; Zech et al. 2015);  $D_m \ll \alpha_L v$ ;  
104 and for  $C_F$  values ranging between 0.01 and 0.1, Equation 6 can be given in a comparative form to  
105 Equation 7, as:

$$106 \quad F \approx -\alpha_L \ln C_F. \quad (8)$$

107

## 108 Numerical Simulations

109

110 FEFLOW (Diersch 2014) was used to simulate 2D steady-state solute transport within a uniform  
111 flow field to provide a simple test case to apply the analytical solutions (in this case, Equation 6).  
112 The model domain was 10 m in the  $x$ -direction and 5 m in the  $y$ -direction and was discretized with  
113 ~100,000 quadrilateral elements. Groundwater flow towards a region of constant concentration ( $C$   
114 = 1) was simulated with  $v = 0.33$  m/d. Upstream and downstream boundaries were represented  
115 with constant concentration ( $C = 0$ ).  $D_{\text{aq}}$  was set at  $8.64 \times 10^{-5}$  m<sup>2</sup>/d,  $\alpha_L$  was 0.1 m and the transverse  
116 dispersivity ( $\alpha_T$ ) was 0.025 m. These dispersivity values are within the plausible range for the scale  
117 of the problem (i.e., Gelhar et al. 1992; Zech et al. 2015).

118

## 119 Results and Discussion

120

### 121 Assessing Upstream Dispersion Effects in Previous Studies

122

123 There are numerous examples in the literature of solute transport problems where groundwater  
124 flows in the direction of increasing concentration, and where models have been applied to analyze  
125 concentration distributions and/or solute fluxes. For the most part, these involve flow and transport  
126 in 2D or 3D, rather than the 1D basis for the previous equations. Nonetheless, the conditions along  
127 flow lines are considered to allow for a first-order approximation of upstream dispersion using the  
128 1D equations given above. This allows for testing of whether upstream dispersion is predictable  
129 under the simplifying assumptions that led to the previous equations. A selection of cases is  
130 presented in Table 1 representing a variety of solute transport situations and scales of analysis.



131 Only brief descriptions of the cases are provided. The reader is directed to the respective references  
 132 for further details.

133

134 **Table 1** Parameter sets used to estimate steady-state upstream dispersion.

Case	$\nu$ (m/d)	$D_{aq}$ (m <sup>2</sup> /d)	$\alpha_L$ (m)	$L$ (m)	$C_F$ (-)	$F^*$ (m)	$F_{(6)}$ (m)	$F_{(7)}$ (m)
Henry (1964)	34.6	1.629	0	2	0.1	0.10	–	0.11
Sebben and Werner (2016) <sup>1</sup>	305	0	0.005	0.583	0.02	0.02	0.023	0.023
Liggett et al. (2014) <sup>2</sup> :								
Very Low $D_L$	0.1	$8.64 \times 10^{-6}$	0.1	~8	0.01	$0.15^3$	–	0.46
Low $D_L$	0.1	$8.64 \times 10^{-5}$	0.1	~8	0.01	$0.15^3$	–	0.46
Intermediate $D_L$	0.1	$8.64 \times 10^{-5}$	1	~8	0.01	$0.31^3$	–	4.6
High $D_L$	0.1	$8.64 \times 10^{-5}$	10	~8	0.01	$0.80^3$	–	46

135  $F^*$  is upstream dispersion estimated from solute transport models.

136  $F_{(6)}$  and  $F_{(7)}$  refer to upstream dispersion from Equations 6 and 7, respectively.

137 <sup>1</sup>Sebben and Werner (2016) results are taken from “Case A1”.

138 <sup>2</sup>Liggett et al. (2014) results are taken from the concave hillslope case “A+Disp”.

139 <sup>3</sup>Transient results, i.e., steady-state conditions were not reached.

140

141 The Henry (1964) problem is a commonly applied 2D benchmark case for evaluating density-  
 142 dependent flow and transport codes. Fresh groundwater enters a 2 m by 1 m coastal aquifer cross  
 143 section and exits through the upper 0.47 m of the vertical sea boundary, as discernible from flow  
 144 lines constructed by Henry (1964). The specified concentration boundary conditions representing

145 the sea induces upstream dispersion, to the degree given as  $F^*$  (obtained at the mid-point of the  
146 outflow face) in Table 1. Application of Equation 7 provides a close match to the upstream  
147 dispersion of the Henry (1964) problem, despite its complex density-dependent conditions.

148

149 Sebben and Werner (2016) studied the influence of discrete flow features (e.g., fractures, faults)  
150 on the characteristics of steady-state solute plumes in otherwise permeable aquifers. Preferential  
151 flow in these features creates conditions where matrix flow occurs in the direction of low-to-high  
152 solute concentrations, leading to anomalous solute concentrations in a selection of cases. Sebben  
153 and Werner (2016) were unable to justify the anomalous solute concentrations, and hypothesized  
154 that “back dispersion” (i.e., upstream dispersion) was the cause. Table 1 provides an estimate of  
155 the extent of upstream dispersion encountered in “Case A1” from Sebben and Werner (2016). Both  
156 Equations 6 and 7 provide close estimates of the extent of upstream dispersion that was produced  
157 in their numerical experiment.

158

159 Liggett et al. (2014) studied the transfer of solutes from the surface to the subsurface in 2D hillslope  
160 catchments using the numerical modeling code HydroGeoSphere (Therrien et al. 2006) to explore  
161 the contributions of event and pre-event water to runoff. Their study investigated various transport  
162 mechanisms (i.e., advection only, advection and dispersion, etc.). Here we assess the cases that  
163 considered advection and dispersion (“A+Disp” in Liggett et al. (2014)). Their models showed  
164 dilution of pre-event water (i.e., due to inflows of event water) in the shallow subsurface that was  
165 attributed to upstream dispersion, which also led to significant errors in solute fluxes to the land  
166 surface. By scaling from their diagrams of concentration distributions, the extent of upstream  
167 dispersion (i.e.,  $F^*$  in Table 1) was estimated.

168

169 Upstream dispersion values obtained from Equation 7, as given in Table 1, are considerably larger  
170 than those observed by Liggett et al. (2014). This is attributable to the transient nature of their  
171 experiments, in contrast to the steady-state assumption of Equation 7. Given that  $F^* < F_{(7)}$  (see  
172 Table 1), it is expected that the simulated (and anomalous) dilution of pre-event water in discharge  
173 areas of the models from Liggett et al. (2014) would continue to grow if simulation times were  
174 extended. The upstream dispersion ( $F^*$  in table 1) in the Liggett et al. (2014) study increased as  
175 the subsurface  $\alpha_L$  increased, as expected from the theory presented herein.

176

177 Upstream dispersion has been reduced or eliminated by modifying the downstream boundary  
178 condition, in a selection of situations. For example, Liggett et al. (2014) modified the surface-  
179 subsurface interface conditions to avoid imposing surface solute concentrations to the upper  
180 boundary of the subsurface. The original Henry (1964) problem has also been changed so that  
181 concentrations along the sea boundary represent that of discharging groundwater in regions of  
182 outflow (Croucher and O'Sullivan 1995).

183

184 Konikow (2011) highlights that a better governing equation of solute transport would solve several  
185 issues that arise from use of the ADE, including unrealistic upstream dispersion. He cites mass-  
186 transfer models (e.g., Haggerty and Gorelick 1995) and continuous time random walk models (e.g.,  
187 Berkowitz et al. 2006) as steps in the right direction. However, he also notes that these approaches  
188 either require additional data, or include parameters that are either non-intuitive, or difficult to  
189 measure. Given the control of  $\alpha_L$ , we suggest that it is possible to limit the extent of upstream

190 dispersion by reducing the hydrodynamic dispersion adopted in models in regions where  
191 groundwater flows in the direction of increasing solute concentration, i.e., through lowering  $\alpha_L$ .

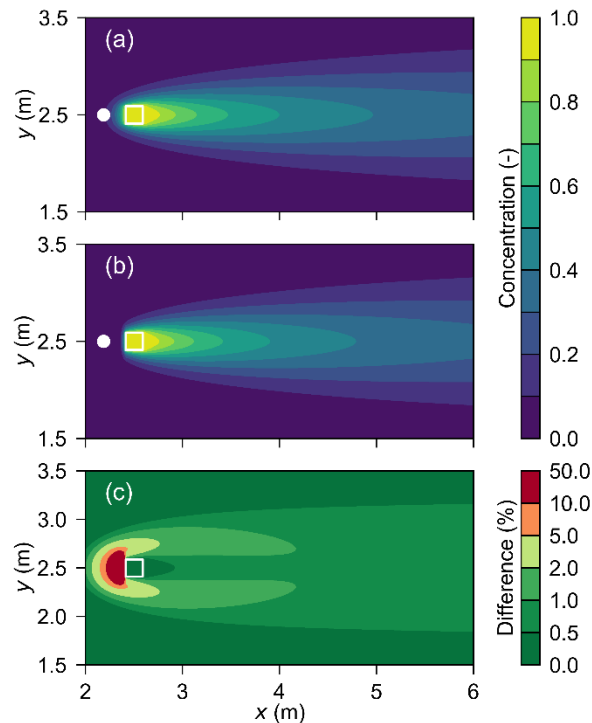
192

### 193 **Simple Approach to Minimize Upstream Dispersion**

194

195 Here, we propose an approach, using the traditional ADE implemented in most models capable of  
196 simulating solute transport. Our approach utilizes Equation 6 or 7 to determine the likely upstream  
197 dispersion, then places a region of low  $\alpha_L$  within this zone. The approach is simple to implement  
198 and the scale over which unrealistic upstream dispersion would have occurred can be quantified.

199 An example of a simulation with no low-dispersivity zone is shown in Figure 1a and with the low-  
200 dispersivity zone in Figure 1b.



201

202 **Figure 1.** Demonstration of the applicability of Equation 6. White square denotes zone of constant  
203 concentration. White circle (Figure 1a, 1b) denotes distance of the 0.1 isochlor as predicted by

204 Equation 6. (a) Model run where  $\alpha_L = 0.1$  m and  $\alpha_T = 0.025$  m. (b) Model modified to include a  
205 zone where  $\alpha_L = \alpha_T = 0.025$  m immediately upstream of the constant concentration zone. (c)  
206 Concentration difference (%) between Figure 1a and 1b. Only a subset of the modelling domain is  
207 shown, to enhance visual inspection of local-scale phenomena. The model domain was  $10 \text{ m} \times 5$   
208 m in the  $x$  and  $y$  directions, respectively.

209

210 Figure 1 shows that unrealistic upstream dispersion can be easily eliminated in numerical  
211 simulation by lowering dispersion parameters immediately upstream of the solute source,  
212 producing minimal changes to the solute transport patterns downstream of the region of lowered  
213 dispersion that would otherwise have occurred. It is worth noting that the results in Figure 1a and  
214 1b are similar to conceptual diagrams in Konikow (2011). Also, implementing the change to the  
215 model had some influence on the downstream concentrations (Figure 1c).

216

217 In this simple application, the lowest possible dispersivity that allows numerically stable results  
218 (i.e.,  $\Delta x / \alpha_L \leq 2$ , where  $\Delta x$  is the spatial discretization) was used for four elements upstream of the  
219 constant concentration zone, although the results are similar to the use of a single row of reduced-  
220 dispersivity elements. This simple approach is intuitive and can be easily implemented in most  
221 numerical model codes, even in cases where the mean flow direction varies in time. For example,  
222 a zone of lower  $\alpha_L$  could be placed around the zone of constant concentration. Reducing the value  
223 of  $\alpha_L$  close to a solute source is also consistent with its apparent spatial variability (e.g., Gelhar et  
224 al. 1992; Zech et al. 2015).

225

226 **Conclusions**

227

228 Upstream dispersion, the unrealistic movement of solutes in the opposite direction to groundwater  
229 flow caused by Fickian dispersion model assumptions in solute transport models, has been  
230 identified in a number of previous studies. Yet there has been no previous guidance for solute  
231 transport modelers to obtain rapid estimates of its likely steady-state extent. In this study, the one-  
232 dimensional advection-dispersion equation for steady-state conditions is solved to produce two  
233 rudimentary solutions for the extent of upstream dispersion under either Dirichlet or Cauchy  
234 boundary conditions at the upstream boundary. Unsurprisingly, upstream dispersion is shown to  
235 be proportional to the dispersivity under common situations. The utility of the new upstream  
236 dispersion equations is demonstrated by application to several complex problems in which  
237 upstream dispersion is either well-matched or the equations at least provide useful insights into the  
238 potential scale of steady-state upstream dispersion effects. We also provide a simple and intuitive  
239 approach to reduce unrealistic upstream dispersion, whereby a reduced value of dispersivity is  
240 applied to a region immediately upstream of the solute source.

241

## 242 **Acknowledgments**

243

244 The authors gratefully acknowledge productive discussions on upstream dispersion with Neville  
245 Robinson and Megan Sebben. The data used are listed in the references and tables. Adrian Werner  
246 is supported by the Australian Research Council's Future Fellowship scheme (project number  
247 FT150100403). Amir Jazayeri is funded by the Australian Research Council (project numbers  
248 FT150100403 and LP140100317). Yu Ye is supported by the National Natural Science Foundation  
249 of China (project number 51709085).

250

251 **References**

252

253 Barbour, S.L., M.J. Hendry, and L.I. Wassenaar. 2012. In situ experiment to determine advective-  
254 diffusive controls on solute transport in a clay-rich aquitard. *Journal of Contaminant*  
255 *Hydrology* 131: 79–88. <https://doi.org/10.1016/j.jconhyd.2011.12.002>

256 Berkowitz, B., A. Cortis, M. Dentz, and H. Scher. 2006. Modeling non-Fickian transport in  
257 geological formations as a continuous time random walk. *Reviews of Geophysics* 44:  
258 RG2003. <https://doi.org/10.1029/2005RG000178>

259 Chen, J.-S., C.-W. Liu, C.-S. Chen, and H.-D. Yeh. 1996. A Laplace transform solution for tracer  
260 tests in a radially convergent flow field with upstream dispersion. *Journal of Hydrology* 183:  
261 263–275. [https://doi.org/10.1016/0022-1694\(95\)02972-9](https://doi.org/10.1016/0022-1694(95)02972-9)

262 Croucher, A.E., and M.J. O’Sullivan. 1995. The Henry problem for saltwater intrusion. *Water*  
263 *Resources Research* 31: 1809–1814. <https://doi.org/10.1029/95WR00431>

264 Cvetkovic, V. 2013. How accurate is predictive modeling of groundwater transport? A case study  
265 of advection, macrodispersion, and diffusive mass transfer at the Forsmark site (Sweden).  
266 *Water Resources Research* 49: 5317–5327. <https://doi.org/10.1002/wrcr.20429>

267 Di Donato, G., E. Obi, and M.J. Blunt. 2003. Anomalous transport in heterogeneous media  
268 demonstrated by streamline-based simulation. *Geophysical Research Letters* 30: 1608.  
269 <https://doi.org/10.1029/2003GL017196>

270 Diersch, H.-J. G. 2014. FEFLOW: Finite Element Modeling of Flow, Mass and Heat Transport in  
271 Porous and Fractured Media. eBook: Springer.

272 Gelhar, L.W., C. Welty, and K.R. Rehfeldt. 1992. A critical-review of data on field-scale  
273 dispersion in aquifers. *Water Resources Research* 28, no. 7: 1955–1974.  
274 <https://doi.org/10.1029/92WR00607>

275 Haggerty, R., and S.M. Gorelick. 1995. Multiple-rate mass transfer for modeling diffusion and  
276 surface reactions in media with pore-scale heterogeneity. *Water Resources Research* 31, no.  
277 10: 2383–2400. <https://doi.org/10.1029/95WR10583>

278 Henry, H.R. 1964. Effects of dispersion on salt encroachment in coastal aquifers. U.S. Geological  
279 Survey Water Supply Paper, 1613-C.

280 Knight, A.C., A.D. Werner, and D.J. Irvine. 2019. Combined geophysical and analytical methods  
281 to estimate offshore freshwater extent. *Journal of Hydrology* 576: 529–540.  
282 <https://doi.org/10.1016/j.jhydrol.2019.06.059>.

283 Konikow, L.F. 2011. The secret to successful solute-transport modeling. *Ground Water* 49: 144–  
284 159. <https://doi.org/10.1111/j.1745-6584.2010.00764.x>

285 Liggett, J. E., A.D. Werner, B.D. Smerdon, D. Partington, and C.T. Simmons. 2014. Fully  
286 integrated modeling of surface-subsurface solute transport and the effect of dispersion in  
287 tracer hydrograph separation. *Water Resources Research* 50: 7750–7765.  
288 <https://doi.org/10.1002/2013WR015040>

289 Liu, G., C. Zheng, and S.M. Gorelick. 2004. Limits of applicability of the advection-dispersion  
290 model in aquifers containing connected high-conductivity channels. *Water Resources*  
291 *Research* 40: W08308. <https://doi.org/10.1029/2003WR002735>

292 Neuman, S.P. 1990. Universal scaling of hydraulic conductivities and dispersivities in geologic  
293 media. *Water Resources Research* 26, no. 8: 1749–1758.  
294 <https://doi.org/10.1029/WR026i008p01749>.



295 Robinson, N.I., J.M. Sharp, and I. Kreisel. 1998. Contaminant transport in sets of parallel finite  
296 fractures with fracture skins. *Journal of Contaminant Hydrology* 31: 83–109.  
297 [https://doi.org/10.1016/S0169-7722\(97\)00055-7](https://doi.org/10.1016/S0169-7722(97)00055-7)

298 Schulze-Makuch, D. 2005. Longitudinal dispersivity data and implications for scaling behavior.  
299 *Ground Water* 43, no. 3: 443–456. <https://doi.org/10.1111/j.1745-6584.2005.0051.x>

300 Sebben, M.L., and A.D. Werner. 2016. A modeling investigation of solute transport in permeable  
301 porous media containing a discrete preferential flow feature. *Advances in Water Resources*  
302 94: 307–317. <https://doi.org/10.1016/j.advwatres.2016.05.022>

303 Therrien, R., R.G. McLaren, E.A. Sudicky, and S.M. Panday. 2006. HydroGeoSphere. Waterloo,  
304 Canada: Groundwater Simulations Group, University of Waterloo.

305 Wooding, R.A., S.W. Tyler, and I. White. 1997. Convection in groundwater below an evaporating  
306 salt lake: 1. Onset of instability. *Water Resources Research* 33: 1199–1217.  
307 <https://doi.org/10.1029/96WR03533>

308 Xu, M.J., and Y. Eckstein. 1995. Use of weighted least-squares method in evaluation of the  
309 relationship between dispersivity and field-scale. *Ground Water* 33, no. 6: 905–908.  
310 <https://doi.org/10.1111/j.1745-6584.1995.tb00035.x>

311 Zech, A., S. Attinger, V. Cvetkovic, G. Dagan, P. Dietrich, A. Fiori, Y. Rubin, and G. Teutsch.  
312 2015. Is unique scaling of aquifer macrodispersivity supported by field data? *Water*  
313 *Resources Research* 51, no. 9: 7662–7679. <http://doi.org/10.1002/2015WR017220>

314 Zhang, Y., C.T. Green, and G.R. Tick. 2015. Peclet number as affected by molecular diffusion  
315 controls transient anomalous transport in alluvial aquifer-aquitard complexes. *Journal of*  
316 *Contaminant Hydrology* 177–178: 220–238. <https://doi.org/10.1016/j.jconhyd.2015.04.001>

317